Hindawi
Geofluids
Volume 2022, Article ID 5828684, 9 pages
https://doi.org/10.1155/2022/5828684

Research Article

Study on Flow Model and Flow Equation of Shale Gas Based on Microflow Mechanism

Huaxun Liu,[1] Shusheng Gao,[1] Feifei Fang,[2] Chunyan Jiao,[1] Liyou Ye,[1] Jie Zhang,[2] and Weiguo An[1]

[1]*PetroChina Research Institute of Petroleum Exploration and Development, Beijing 100083, China*
[2]*School of Petroleum Engineering, Chongqing University of Science and Technology, Chongqing 401331, China*

Correspondence should be addressed to Feifei Fang; fangfeifei@cqust.edu.cn
and Chunyan Jiao; jiaochunyan69@petrochina.com.cn

Received 10 December 2021; Accepted 25 August 2022; Published 20 September 2022

Academic Editor: Zhiming Chen

Shale gas storage and permeability space is between nanometers and micrometers and has strong multiscale characteristics, resulting in highly complicated shale gas flow. Therefore, the development of shale gas needs to clarify the seepage mechanism of shale gas and establish a flow model and flow equation that can analyze shale gas flow. In this paper, based on the single nanotube model, combined with the Weiyuan-Changning shale gas demonstration zone of the target layer of the Longmaxi formation shale core high-pressure mercury pore throat test results, the contribution of seepage, diffusion, transition flow, and free molecular flow to shale gas flow was calculated. The contribution of seepage and diffusion is over 95%, and seepage and diffusion are the main flow pattern. Then, a shale gas seepage and diffusion coupled flow model and coupled flow equation were established. A method for calculating shale permeability and diffusion was proposed using the relationship between flow pressure and shale gas velocity. Finally, shale gas flow experiment analysis was carried out to verify that the established shale gas flow model and flow equation can describe the shale gas flow well. The result shows that the flow rate of shale gas is composed of seepage flow rate and diffusion flow rate. The seepage flow rate is proportional to the pseudopressure difference and proportionate to the low-pressure squared difference. The diffusion velocity is proportional to the difference in shale gas density, and the pressure difference in low pressure is proportional. As the pressure of a shale gas reservoir decreases, the proportion of diffusion flow increases. The research results enrich the understanding of shale gas flow; it also has particular reference significance to the development of shale gas reservoirs.

1. Introduction

The continuous deepening of oil and gas exploration and development increases reserves and production of conventional oil and gas resources [1]. The strategic position of unconventional oil and gas resources has become more critical and has gradually become replacement energy for conventional oil and gas resources [2]. As an important unconventional oil and gas resource, shale gas is widely used in China and has great development potential [3, 4]. Shale pore throat is tiny, mostly nanoscale pore throat. Gas flowing in the nanopore throat is different from that of the conventional pore throat, which has a microscale effect and includes seepage, diffuse, transitional flow, and free molecular flow [5, 6]. Therefore, confirming the seepage mechanism and law of clear shale gas and constructing the corresponding seepage model accordingly are of great significance to the efficient development of shale gas.

At present, the research on shale gas seepage mainly focuses on flow experiments and theory methods. Gao et al. [7] studied shale gas flow by flow experiments. Based on the capillary model and citing solid deformation theory, Shen et al. [8] studied the dynamic characteristics of gas molecules percolating in nanoscale pores. Yao et al. [9] learned shale gas flow and gave shale gas flow by Boltzmann method or Knudsen law. Geng et al. [3], under the assumption of ignoring adsorption and desorption, established a flow model that can describe the continuous flow state, slip

flow state, transition state, and molecular state of the gas in shale nanopore throats. Sun et al. [10], considering the effects of multicomponent slip flow and Knudsen diffusion, proposed a new model for simulating the transport of multicomponent shale gas through nanopores in shale formations. Li et al. [11] used multiple relaxation time lattice Boltzmann method (LBM) simulations to study the flow characteristics of shale gas in sudden and gradual contraction channels and explored the influence of Knudsen number and cross-sectional contraction coefficient on shale gas transportation. Foroozesh et al. [12] used the pore network model to study shale gas reservoirs' slip and gas desorption. Le et al. [13] developed a new calculation model for coupled airflow in hydraulic fractures and porous shale matrix within a multiscale modelling framework. Based on the shale model obtained by physical experiments, Chen et al. [14] used the MINC-EDFM coupling method to analyze the comprehensive sensitivity factors of the shale gas-water two-phase fracturing production process, including nanopore radius, nonideal gas effects, and adsorption. Hu and Wang [15] proposed a modified lattice Boltzmann model with effective relaxation time to simulate the microflow behavior of shale gas in fractal organic matter and predict reservoir permeability.

Although these studies emphasize various forms of flow in shale, in the analysis of shale gas flow, the pore throat radius is assumed to be the same or a single flow pattern [16–21]. Significantly, the report about how to obtain shale coupled flow parameters by the experimental method is little, receiving shale permeability and diffusion coefficient from seepage model and diffusion model, respectively, without consideration of the coupling process of shale gas flow [22–24]. In this paper, first, the contribution rates of various flow patterns to the shale gas flow rate are calculated, and the main flow patterns are analyzed of shale gas. Then, a shale gas flow model was established, the coupled flow equation of shale gas was deduced, and the calculation method of permeability and diffusion coefficient was proposed. These calculation methods determine the coupled flow capacity of shale gas. The research results enrich the understanding of shale gas flow, solve the problem about the calculation of the shale coupled flow parameters, and have particular reference significance to the development of shale gas reservoirs.

2. Shale Gas Coupled Flow Model

Nanopore throat is dominantly developed in shale; gas flowing in shale has a microscale effect. Knudsen number (K_n) is a characteristic parameter of microscale flow. Define the ratio of the molecular mean free path to the flow characteristic length [22]:

$$K_n = \frac{\lambda}{d}, \tag{1}$$

where d is the pore throat diameter (nm) and λ is the molecular mean free path (nm). λ formulation is given by

$$\lambda = \frac{\kappa_B T}{\sqrt{2}\pi {\delta_m}^2 P_m}, \tag{2}$$

where k_B is the Boltzmann constant, 1.3805×10^{-23} J/K; T is the temperature, K; P_m is the average gas pressure, MPa; and δ_m is the gas molecular diameter, nm, in which methane molecular free path in standard state is 40 nm.

Gas flow can be divided into four modes by K_n. No-slip flow: $K_n < 0.001$, fluid can be regarded as a continuous medium and flow is no-slip flow, the flow can be described by the Navier-Stokes (N-S) equation with no slip. It is generally considered this flow as a seepage in porous media, which follows Darcy's law, and flow equation [23]

$$q_{1m} = A\frac{K}{\mu B_g}\rho_{sc}\frac{\partial P}{\partial x}. \tag{3}$$

The continuous flow of slip: $0.001 < K_n < 0.1$ have a microscale effect, and fluid can also be regarded as a continuous medium. There has a strong slip effect in the boundary, and the flow can be described by the Navier-Stokes (N-S) equation with boundary effect. It is generally considered this flow as diffusion in porous media, which follows Fick's law, and flow equation [22]

$$q_{2m} = AD\frac{\partial C}{\partial x}. \tag{4}$$

Transitional flow: $0.1 < K_n < 10$, the continuous medium assumption is not appropriate, and the Burnett equation can describe the flow. Free molecular flow: $K_n > 10$, researchers study the flow by molecular dynamics method.

Yao et al. [9] presented that the flow capacity of pore throat can be described by equivalent permeability and gave equivalent permeability formulation:

$$K_n = \frac{r^2}{8}\left(1 + \frac{6K_n}{1 + K_n}\right). \tag{5}$$

Therefore, the contribution of pore throat (radius r_i) in total flowing

$$f(r_i) = \frac{\Delta S_i\left(r_i^2/8\right)\left(1 + \left(6K_n/\left(1 + K_n\right)\right)\right)}{\sum_{j=1}^{n}\Delta S_j\left(r_j^2/8\right)\left(1 + \left(6K_n/\left(1 + K_n\right)\right)\right)} \times 100. \tag{6}$$

The Changning-Weiyuan area is China's current shale gas field with the largest reserves and production, and it is also a national-level shale gas field test area. The shale reservoirs in this area are very representative. To determine the contribution of the four flow patterns to shale gas flow, we selected six shale rocks from the Changning-Weiyuan national demonstration area of shale gas (permeability 0.004~0.02 mD, porosity 1.8~3.3%) and tested the radius of pore throat by high-pressure mercury. Maximum mercury intake pressure is approximately 400 MPa and can identify the pore throat which radius is larger than 2 nm. Figure 1 shows the cumulative distribution curve of the pore throat radius. Figure 2 shows the cumulative contribution of pore throat flow (from the

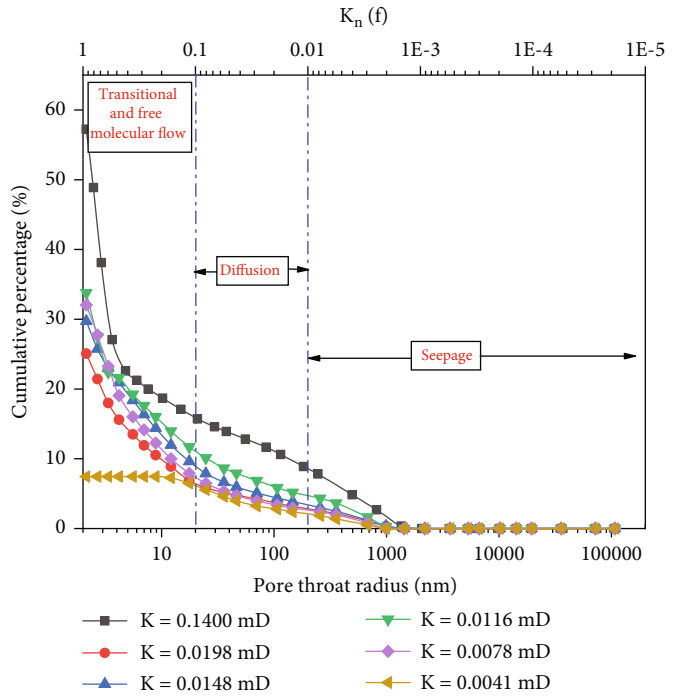

Figure 1: Cumulative distribution curve of pore throat radius.

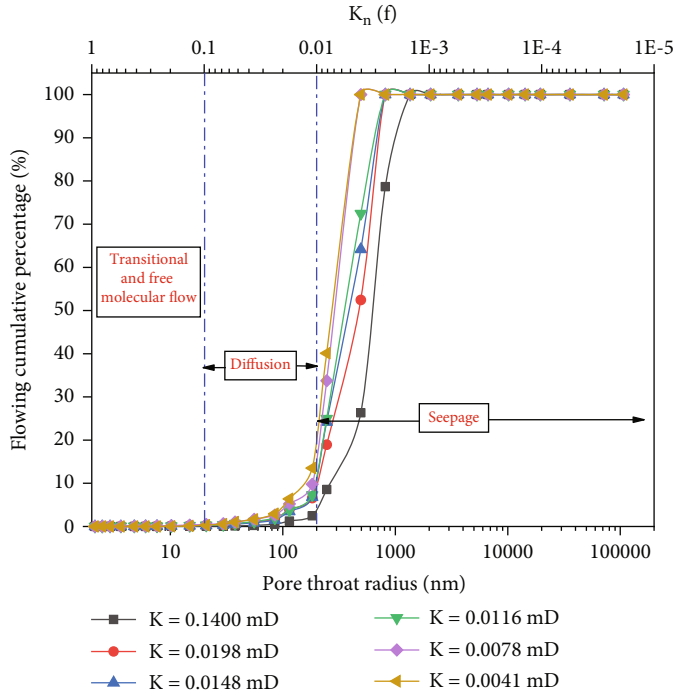

Figure 2: Cumulative contribution of pore throat flow.

minimum size of pore throat). The Knudsen number at 1 MPa flow pressure is given in the picture.

Comparing Figures 1 and 2 shows that shale pore throat is very small, and the pore throat radius over 200 nm (K_n less than 0.01, seepage) accounts for 1.8~7.9%, average 3.7%. The contribution of flow accounts for 67~93%, an average of 83%, a small proportion of pore throat flowing belongs to seepage. Still, this proportion of pore throat belongs to the dominant channel and accounts for the maximum proportion of shale gas flow, so seepage is the main flow pattern from the contribution of shale gas flow. Pore throat with a radius of between 20 and 200 nm (K_n: 0.01~0.1, diffusion) accounts for 3~8%, average 3.7%, the contribution of flow accounts for 6~22%, intermediate

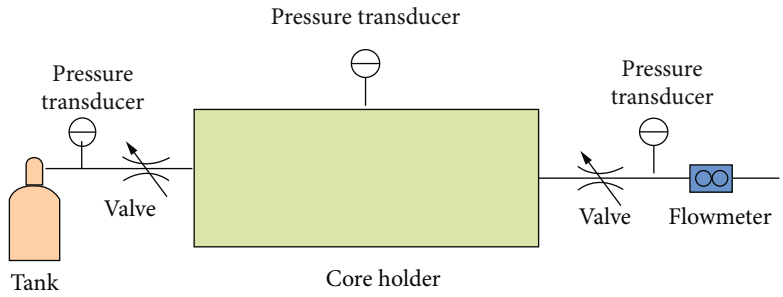

Figure 3: Sketch map of shale gas flow.

16.5%, a little proportion of pore throat flowing belongs to diffusion, but diffusion is a vital flow pattern from the contribution of shale gas flow. Most pore throat radius less 20 nm (K_n over 0.1) accounts for 90%, and most pore throat flows are transitional or free molecular flows. But the contribution of flow only accounts for 0.5%, and it can be ignored. So considering from the contribution of flow, seepage and diffusion are the main flow pattern of shale gas, the flow model can be expressed [24]

$$q_m = A\frac{K}{\mu B_g}\rho_{sc}\frac{\partial P}{\partial x} + AD\frac{\partial C}{\partial x}, \tag{7}$$

where q_m is the shale gas flow rate, mg/s. The first right item in the formula is the seepage flow rate, and the second is the diffusion flow rate.

3. Shale Gas Flow Equation and Parameter Inversion Method

3.1. Physical Model. Shale gas flow is the linear flow of vertical fracture after volume fracturing; shale gas flow can be recognized by studying linear flow. According to the flow mentioned above mechanism and the results of model research, these assumptions are given about shale gas flow:

(1) Flow belongs to linear, isothermal, and stable flow. The flow line distance is L, the cross-sectional area is A, the inlet pressure is P_1, and the outlet pressure is P_2, as shown in Figure 3

(2) Seepage and diffusion are the main flow pattern of shale gas, seepage follows Darcy's law, and diffusion follows Fick's law

3.2. Mathematical Model and Derivation. Considering such as shale gas flow physical model of the 2.1 hypothesis, shale gas flow rate q_m can be expressed by equation (7), rewritten in the form, introducing gas state equation

$$B_g = \frac{ZTP_{sc}}{T_{sc}P}, \tag{8}$$

$$C = \phi\frac{PM}{ZRT}, \tag{9}$$

where P_{sc} is the standard atmospheric pressure, 0.101 MPa. T_{sc} is the standard temperature, 273.15 K. T is the formation or flow experiment temperature, K. Z is the gas compressibility factor. M is the gas molecular weight. R is the gas constant, 8.314 J/(mol·K), and Φ is the shale porosity.

Bring equations (8) and (9) into equation (7), shale gas mass flow q_m can be expressed in the form

$$q_m = \frac{AT_{sc}K}{T}\frac{P}{\mu Z P_{sc}}\rho_{sc}\frac{\partial P}{\partial x} + \frac{A\phi DM}{RT}\frac{\partial}{\partial x}\left(\frac{P}{Z}\right). \tag{10}$$

Introducing pseudopressure function β and density function δ, expressions are as follows:

$$\beta = 2\int_{P_{sc}}^{P}\frac{p}{\mu Z}dp, \tag{11}$$

$$\delta = \int_{p_{sc}}^{P}\frac{\phi M}{ZRT}dp. \tag{12}$$

Bring equations (11) and (12) into equation (10), shale gas flow q_m also can be expressed in the form from integral of equation (10):

$$q_m = \frac{A\rho_{sc}T_{sc}K}{2LTP_{sc}}(\beta_1 - \beta_2) + \frac{AD(\delta_1 - \delta_2)}{L}, \tag{13}$$

where β_1 is the inlet pseudopressure, MPa^2/(mPa·s). β_2 is the inlet pseudopressure, MPa^2/(mPa·s). δ_1 is the inlet density, kg/m^3. δ_2 is the outlet density, kg/m^3. Equation (11) shows that shale flow consists of seepage flow rate and diffusion flow rate. The seepage flow rate is proportional to the pseudopressure difference between inlet and outlet. The diffusion flow rate is proportional to the density difference between the inlet and the outlet.

In addition, according to the analysis of the gas high-pressure physical property, gas viscosity and compressibility factor are almost constant when the pressure is low. For example, methane viscosity (ranged from 0.018 to 0.019 mPa·s) and compressibility factor (ranged from 0.99 and 1.00) are almost constant if pressure is less than 10 MPa. The temperature is room temperature, about 25 degrees Celsius. Thus, equation (11) can be modified further and replaced the expression

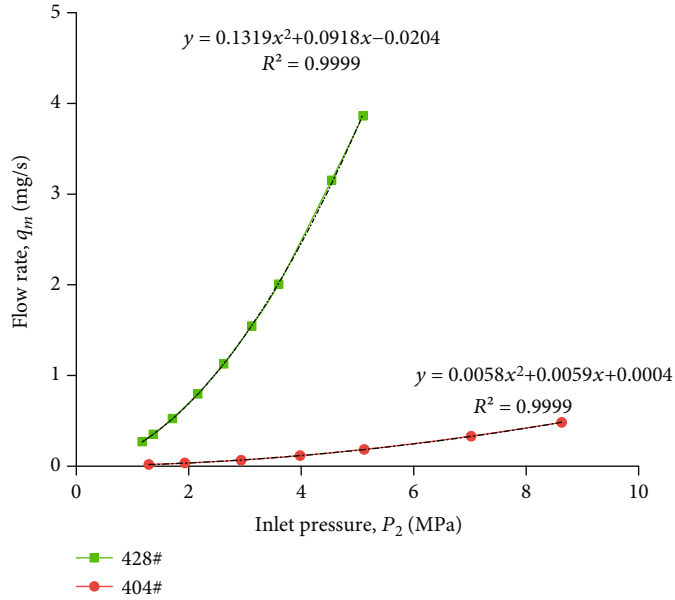

Figure 4: Shale gas flow characteristic curve.

$$q_m = \frac{A\rho_{sc}T_{sc}K}{2\mu ZLTP_{sc}}\left(P_1^2 - P_2^2\right) + \frac{\phi ADM(P_1 - P_2)}{ZRTL}. \quad (14)$$

Shale gas flow rate under low pressure can also be expressed by equation (14), which shows that seepage flow rate is proportional to pressure square difference between inlet and outlet. The diffusion flow rate is proportional to the pressure difference between inlet and outlet when shale flows in low-pressure formation. Shale gas flow patterns can be determined by the relationship between shale gas flow rate and the pressure difference or pressure square difference between inlet and outlet. Seepage and diffusion are the main flow patterns when shale gas flow is proportional to pressure square and pressure difference, respectively.

If outlet pressure is constant pressure, for example, outlet pressure is usually standard atmospheric pressure ($P_2 = 0.101$ MPa) when shale gas displacement experiments are taken in the laboratory. The relationship between shale gas flow and inlet pressure is the binomial relationship; permeability K and diffusion coefficient D can be given from the binomial fitting between shale gas flow and inlet pressure; specific expressions are as follows:

$$K = \frac{2\mu ZLTP_{sc}}{A\rho_{sc}T_{sc}}a, \quad (15)$$

$$D = \frac{ZRTL}{\phi AM}b, \quad (16)$$

where a is the two-term coefficient of binomial. b is the one-term coefficient of binomial, as shown in Figure 4.

Further, the contribution of seepage or diffusion to shale gas rate also can be obtained from equation (11) or (12). The right-first item is seepage contribution, and the right-second item is diffusion contribution. Further, it can be determined which flow is the main flow in shale reservoir.

Only considering seepage or Darcy model, equation (14) can be simplified to normal pressure square equation [25]

$$q_m = \frac{A\rho_{sc}T_{sc}K}{2\mu ZLTP_{sc}}\left(P_1^2 - P_2^2\right). \quad (17)$$

Only considering diffusion or Fick diffusion model, equation (14) can be simplified to normal gas diffusion equation [26]

$$q_m = \frac{\phi ADM(P_1 - P_2)}{ZRTL}. \quad (18)$$

4. Case Analysis

We carried out a coupled flow experiment with shale cores at diameter 2.5 cm, selected from Longmaxi formation of the Changning-Weiyuan gas reservoir. The experimental temperature is 26 degrees Celsius. The outlet pressure is the standard atmosphere, tested shale gas flow rate under different inlet pressure. Other experimental parameters, experimental results, and analysis results are shown in Table 1. Due to inlet pressure lower than 10 MPa, gas viscosity and compressibility factor are constant, so shale permeability is calculated according to equation (15) based on the Darcy model. Shale diffusion is calculated according to equation (16) based on the Fick diffusion model; shale permeability and diffusion coefficient by the fitting method are calculated according to equation (12) based on coupled flow model.

Table 1 suggests that the larger the flow pressure is, the smaller the permeability of shale is calculated according to the Darcy model. The larger the diffusion coefficient of shale is calculated according to the Fick diffusion model. Furthermore, the variation of gas permeability and diffusion

Table 1: Results of experimental analysis for shale coupled flow.

Core no.	Length (cm)	Porosity (%)	Inlet pressure (MPa)	Flow rate (mL/s)	Conventional model		Coupled model	
					Permeability (μD)	Diffusion coefficient (mm^2/s)	Permeability (μD)	Diffusion coefficient (mm^2/s)
			1.29	0.0117	1.69	2.7		
			1.93	0.0253	1.63	3.8		
			2.93	0.0562	1.57	5.5		
404	3.21	2.40	3.98	0.0991	1.50	7.0	1.15	1.73
			5.12	0.1575	1.44	8.7		
			7.02	0.2835	1.38	11.3		
			8.63	0.4147	1.33	13.4		
			1.17	0.232	40.9	55.2		
			1.37	0.301	38.6	60.4		
			1.71	0.451	37.1	71.4		
			2.16	0.684	35.2	84.5		
428	2.59	2.60	2.62	0.968	33.8	97.9	27.2	19.0
			3.12	1.327	32.7	111.9		
			3.60	1.722	31.9	125.3		
			4.54	2.706	31.5	155.3		
			5.10	3.316	30.6	169.0		

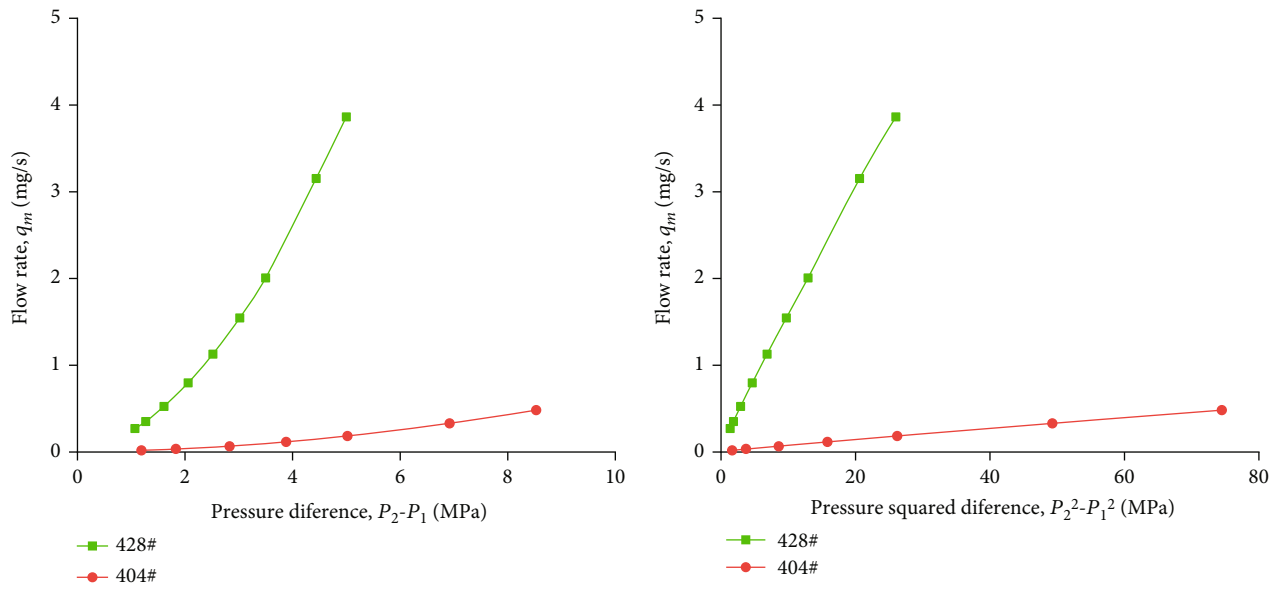

(a) Pressure squared difference

(b) Pressure difference

Figure 5: Shale gas flow test curve.

coefficient under different flow pressure is immense, especially diffusion coefficient. The test results under different flow pressure differ by five times; the permeability variation is also up to 30%. The shale permeability and diffusion coefficient obtained by laboratory experiments cannot be directly applied to the shale reservoir. The conventional and diffusion equations have some limitations in predicting shale gas flow. The relationship between gas rate and pressure difference (pressure square difference) significantly deviates from linear. The former curves fall, the last curve upwards (Figure 5), showing that there are two kinds of flow patterns in shale: seepage and diffusion. And, these two kinds of flow are apparent.

According to the coupled flow equation (i.e., equation (12)), the shale gas flow rate and inlet pressure curve are fitted and analyzed, as shown in Figure 4, and the fitting accuracy is high. The correlation coefficient is close to 1, which suggests that the shale gas flow equation derived in this paper is suitable for the analysis of shale gas flow. Shale permeability K and diffusion coefficient D are calculated by fitting the two terms and the first term coefficient (Figure 4, Table 1). It then calculates the gas flow rate by

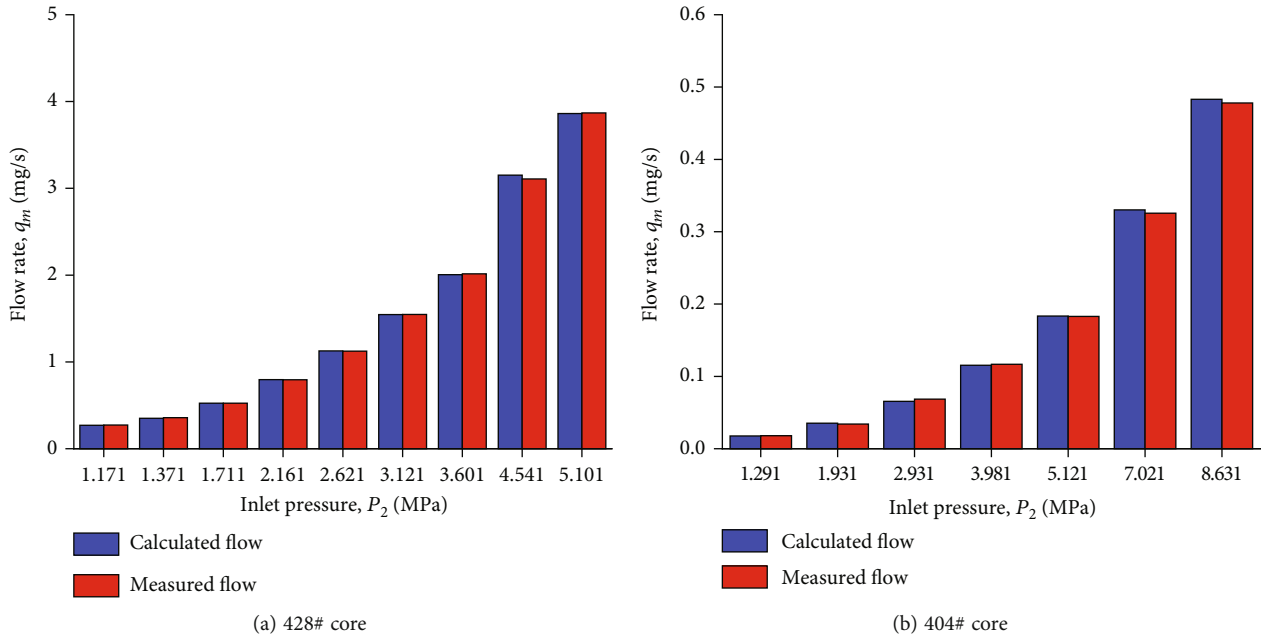

Figure 6: Comparison of calculated and measured flow rates.

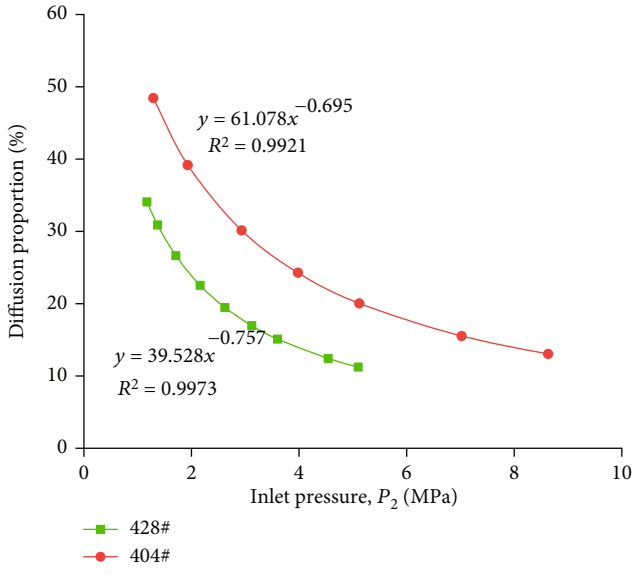

Figure 7: Diffusion's contribution under different inlet pressure.

coupled flow equation (i.e., equation (12)) and compares it with the measured flow rate (Figure 6). It shows that the calculated flow based on the coupled equation agrees with the measured flow. The maximum relative error is 5%, and the vast majority of the error is less than 3% (Figure 6). So, in the analysis and prediction of shale gas flow, it is advisable to use the shale coupled flow equation.

Figure 7 shows the ratio of core diffusion flow to total flow calculated based on the coupled flow model. The figure shows that the ratio of core diffusion mass flow to total mass flow has a power function relationship with flow pressure, and the power exponent is close to -1. Flow pressure significantly influences the proportion of shale diffusion mass flow. For example, the proportion of the diffusion flow rate of the two pieces of shale tested, the proportion of the diffusion mass flow rate under indoor low-pressure conditions (flow pressure less than 1 MPa) is close to 50% or even higher. Therefore, it is necessary to consider the influence of diffusion flow when evaluating the seepage capacity of shale in laboratory experiments. When the flow pressure is greater than 10 MPa, even if the permeability of the two shales tested is micro-Darcy, the diffusion mass flow rate is still less than 10%, which is very small. Under normal conditions, the contribution of diffusion to the flow of shale gas under high pressure in the reservoir is negligible.

Compared with 428# core with 404#, it shows that the larger permeability is, the smaller the diffusion contribution is due to the higher the permeability, the greater number of large pore throat. According to Knudsen's law, shale gas flowing in the large pore throat is seepage, so seepage contribution increases and diffusion contribution decreases with the growth of permeability. This view is consistent with the existing theory. Further, it suggests that our model is suitable.

5. Conclusion

(1) There are four flow patterns (seepage, diffusion, transitional flow, and free molecular flow) in shale, but the effects of these four modes on shale gas flow are different, and the difference is significant. So, when establishing the model of shale gas flow, the main flow pattern should be determined first

(2) Shale permeability and shale diffusion coefficient are obtained by conventional flow equation related to flow pressure, with considerable variation. Calculate

flow based on the coupled flow equation and test flow match well, so we can analyze shale gas flow by coupled flow equation. The permeability and diffusion coefficients obtained from the coupled flow equations are used to characterize the flow capacity of shale reservoirs

(3) Seepage and diffusion are the main flow pattern in domestic developed shale gas reservoirs; the production pressure determines well productivity, and the difference of production squared pressure. The influence of production pressure difference on well productivity increases with the reduction of gas reservoirs pressure

Data Availability

The data used to support the findings of this study are available from the corresponding author upon request.

Disclosure

The abstract for this manuscript was presented at the Inter-Pore 10th Annual meeting and Jubilee, and an earlier version of this manuscript was deposited as a preprint at Research Square [27].

Conflicts of Interest

The authors declare that there are no conflicts of interest regarding the publication of this paper.

Authors' Contributions

This paper is a collaborative work for all the authors. H. X. Liu and S. S. Gao proposed the idea and wrote the manuscript. C. Y. Jiao and J. Zhang established and derived the mathematical model. L. Y. Ye and W. G. An helped with the analysis of the experimental data. J. Zhang and F. F. Fang revised and perfected the paper. All authors have read and agreed to the published version of the manuscript.

Acknowledgments

This work was supported by the CNPC prospective fundamental major scientific and technological projects (2021DJ1701) and the General Program of the Natural Science Foundation of Chongqing (No. cstc2020jcyj-msxmX0659).

References

[1] D. Z. Dong, Y. M. Wang, X. J. Li et al., "Breakthrough and prospect of shale gas exploration and development in China," *Natural Gas Industry B*, vol. 3, no. 1, pp. 12–26, 2016.

[2] Y. S. Ma, X. Y. Cai, and P. R. Zhao, "China's shale gas exploration and development: understanding and practice," *Petroleum Exploration and Development*, vol. 45, no. 4, pp. 589–603, 2018.

[3] Z. Caineng, D. Dazhong, W. Yuman et al., "Shale gas in China: characteristics, challenges and prospects (I)," *Petroleum Exploration and Development*, vol. 42, no. 6, pp. 753–767, 2015.

[4] Z. Caineng, D. Dazhong, W. Yuman et al., "Shale gas in China: characteristics, challenges and prospects (II)," *Petroleum Exploration and Development*, vol. 43, no. 2, pp. 182–196, 2016.

[5] T. Zhong, D. Z. Dong, Y. M. Wang et al., "Characteristics of pore structure of marine shales in South China," *Natural Gas Industry*, vol. 32, no. 9, pp. 1–4, 2012.

[6] X. S. Guo, Y. P. Li, R. B. Liu, and Q. B. Wang, "Characteristics and controlling factors of micropore structures of the Longmaxi Shale in the Jiaoshiba area, Sichuan Basin," *Natural Gas Industry B*, vol. 1, no. 2, pp. 165–171, 2014.

[7] S. S. Gao, W. Xiong, X. G. Liu, Z. M. Hu, and H. Xue, "Experimental research status and several novel understandings on gas percolation mechanism in low-permeability sandstone gas reservoirs," *Natural Gas Industry*, vol. 30, no. 1, pp. 52–55, 2010.

[8] W. J. Shen, X. Z. Li, Y. M. Xu, Y. Sun, and W. Huang, "Gas flow behavior of nanoscale pores in shale gas reservoirs," *Energies*, vol. 10, no. 6, p. 751, 2017.

[9] Y. Jun, Z. Jianlin, Z. Min, Z. Lei, Y. Yongfei, and S. Zhixue, "Microscale shale gas flow simulation based on lattice Boltzmann method," *Acta Petrolei Sinica*, vol. 36, no. 10, pp. 1280–1289, 2015.

[10] F. R. Sun, Y. D. Yao, G. Z. Li, and X. F. Li, "A slip-flow model for multi-component shale gas transport in organic nanopores," *Arabian Journal of Geosciences*, vol. 12, no. 5, pp. 1–11, 2019.

[11] X. Z. Li, J. C. Fan, H. Yu, Y. B. Zhu, and H. A. Wu, "Lattice Boltzmann method simulations about shale gas flow in contracting nano- channels," *International Journal of Heat and Mass Transfer*, vol. 122, pp. 1210–1221, 2018.

[12] J. Foroozesh, A. I. M. Abdalla, and Z. Zhang, "Pore network modeling of shale gas reservoirs: gas desorption and slip flow effects," *Transport in Porous Media*, vol. 126, no. 3, pp. 633–653, 2019.

[13] T. D. Le, M. A. Murad, and P. A. Pereira, "A new matrix/fracture multiscale coupled model for flow in shale-gas reservoirs," *SPE Journal*, vol. 22, no. 1, pp. 265–288, 2017.

[14] S. X. Cheng, P. Huang, K. Wang, K. Wu, and Z. Chen, "Comprehensive modeling of multiple transport mechanisms in shale gas reservoir production," *Fuel*, vol. 277, article 118159, 2020.

[15] B. W. Hu and J. G. Wang, "A lattice Boltzmann simulation on the gas flow in fractal organic matter of shale gas reservoirs," *Journal of Petroleum Science and Engineering*, vol. 210, article 110048, 2022.

[16] K. L. Wu, Z. X. Chen, X. F. Li, C. Guo, and M. Wei, "A model for multiple transport mechanisms through nanopores of shale gas reservoirs with real gas effect-adsorption-mechanic coupling," *International Journal of Heat and Mass Transfer*, vol. 93, pp. 408–426, 2016.

[17] D. Yonggang, C. Tingkuang, Y. Xiaoying, Z. Ying, and W. Guiping, "Simulation of gas flow in nanoscale pores of shale gas deposits," *Journal of Southwest Petroleum University (Science & Technology Edition)*, vol. 37, no. 3, pp. 63–68, 2015.

[18] S. Roy, R. Raju, H. F. Chuang, B. A. Cruden, and M. Meyyappan, "Modeling gas flow through microchannels and nanopores," *Journal of Applied Physics*, vol. 93, no. 8, pp. 4870–4879, 2003.

[19] A. Sakhaee-Pour and S. L. Bryant, "Gas permeability of shale," *SPE Reservoir Evaluation & Engineering*, vol. 15, no. 4, pp. 401–409, 2012.

[20] A. Beskok and G. E. Karniadakis, "REPORT: a model for flows in channels, pipes, and ducts at micro and nano scales," *Microscale Thermophysical Engineering*, vol. 3, no. 1, pp. 43–77, 1999.

[21] F. Javadpour, "Nanopores and apparent permeability of gas flow in mudrocks (shales and siltstone)," *Journal of Canadian Petroleum Technology*, vol. 48, no. 8, pp. 16–21, 2009.

[22] L. Ren, L. Liang, Y. Q. Hu, and J. Z. Zhao, "Analysis of gas flow behavior in nanoscale shale gas reservoir," *Journal of Southwest Petroleum University (Science & Technology Edition)*, vol. 36, no. 5, p. 111, 2014.

[23] T. Y. Yao, Y. Z. Huang, and J. S. Li, "Flow regim for shale gas in extra low permeability porous media," *Chinese Journal of Theoretical and Applied Mechanics*, vol. 44, no. 6, pp. 990–995, 2012.

[24] G. Wei, X. Wei, G. Shusheng, and L. Honglin, "Gas flow characteristics in shales nanopores," *Oil Drilling and Production Technology*, vol. 34, pp. 57–60, 2012.

[25] R. Wang, N. S. Zhang, X. J. Liu, X. M. Wu, and J. Yan, "The calculation and analysis of diffusion coefficient and apparent permeability of shale gas," *Journal of northwest university (Natural science edition)*, vol. 43, no. 1, pp. 75–80, 2013.

[26] S. L. Yang and J. Z. Wang, *Reservoir Physics*, Petroleum Industry Press, Beijing, 2010.

[27] H. Liu, C. Jiao, S. Gao, L. Ye, and W. An, "Study on flow model and flow equation of shale gas based on micro flow mechanism," preprint (version 1) available at Research Square, 2021.